EXPERIMENTAL INVESTIGATIONS ON DYNAMIC CHARACTERISTICS OF A MULTILAYER PIEZOELECTRIC STACK ACTUATOR

Hsien-Yang Lin * **Chien-Ching Ma** **

Department of Mechanical Engineering
National Taiwan University
Taipei, Taiwan 10617, R.O.C.

ABSTRACT

Multilayer piezoelectric stack actuators are widely used in many industrial applications and the investigation on the dynamic behavior of this element is needed. In this study, two optical interferometric techniques called amplitude-fluctuation electronic speckle pattern interferometry (AF-ESPI) and laser Doppler vibrometer (LDV) are used to experimentally investigate the vibration characteristics of a single-layer piezoelectric disc and a multilayer piezoelectric stack actuator. These two techniques are full-field measurement for AF-ESPI and point-wise displacement measurement for LDV. Because the clear fringe patterns obtained by the AF-ESPI method will be shown only at resonant frequencies, both the resonant frequencies and corresponding vibration mode shapes of the piezoelectric disc and the multilayer piezoelectric stack actuator are obtained simultaneously by the AF-ESPI method. Interferometric fringe patterns for both the in-plane and out-of-plane vibration mode shapes are demonstrated. In addition to the proposed two optical techniques, numerical computations based on a commercially available finite element package are presented for comparison with the experimental results. Good agreement between the measured data by experimental methods and the numerical results predicted by FEM is found in resonant frequencies and mode shapes for the single-layer piezoelectric disc. However, some discrepancies are observed for the results obtained by AF-ESPI and impedance analysis for the multilayer piezoelectric stack actuator. A detailed discussion is made to address important issues of this problem.

Keywords : AF-ESPI, Impedance analysis, Piezoelectric disc, Vibration, Resonant frequency, Mode shape.

1. INTRODUCTION

It is well known that piezoceramics, especially the multilayer piezoelectric stack actuators, have been employed in many industrial applications, such as the ultraprecise motion control, laser scanner, power operation with active vibration control, and combustion machine for valve control. Recently, the demand for the multilayer piezoelectric stack actuators has strongly increased because this element provides quick response time, compact, high electromechanical coupling and large generative forces. To exploit the performance of these piezoelectric elements completely, experimental measurement of the response for displacement field is essential. Among the measurement techniques for surface displacements, optical interferometry that uses laser as the light source is the most effective and sensitive method. An increasing trend in applications of optical techniques to obtain the experimental result of multilayer piezoelectric stack actuators is found in many technical literatures. Wolff, *et al.* [1] used a two-channel optical measurement technique based on the Doppler effect to measure the dynamic deflections of PZT multilayer actuators. Damjanovic [2] studied the nonlinearity and hysteresis effects in ferroelectric materials and controlled the piezoelectric nonlinearity and hysteresis by material processing. Janocha and Clephas [3] presented some characteristics for piezoelectric stacks and showed that the behavior of the transducers is strongly dependent on the mechanical and electrical operating conditions. Moilanen and Leppävuori [4] used a developed Michelson interferometric measurement system and Moiré interferometer to measure the out-of-plane displacement responses and to access the edge effects of multilayer devices. Most of the papers mentioned above

* Graduate student ** Professor

concentrate the issues on the point-by-point measurement of displacement response under DC electrical loading for the multilayer piezoelectric stack actuators. However, the detailed studies on the dynamic characteristics of the multilayer piezoelectric stack actuator are limited. There are very few experimental results available for the full-field measurement of surface displacement of piezoelectric elements in resonance. Hence, in this study, we use the full field AF-ESPI optical method to experimentally investigate the resonant frequencies and corresponding mode shapes of a single-layer piezoelectric disc and a multilayer piezoelectric stack actuator under alternating current (AC) electrical loading.

Electronic speckle pattern interferometry (ESPI) is also known as TV-holography or electro-optic holography. It combines the object and reference beams and directs them collinearly towards the detector array of frame-transfer CCD (charge-coupled device), which interfaces to a computer for video electronic processing of speckle patterns, then displays on a TV-monitor in real time (about 30ms). Because the interferometric image is recorded and updated every 1/30s, ESPI is faster and more insensitive to environment than holography. For these reasons, ESPI has become a powerful technique used in many academic researches and engineering applications. Because ESPI uses a video recording and display, its real-time nature makes it practical for vibration measurement. The first recorded work on ESPI was proposed by Butters and Leendertz [5] to investigate the out-of-plane displacement of a vibrating disk. Since then many researches have been forwarded in the area of deformation analysis [6,7], especially for vibration measurement [8~10]. In the effort to increase image contrast, Ma and his coworker [11,12] further developed the amplitude-fluctuation ESPI (AF-ESPI) based on the work in [10]. In their works, AF-ESPI clearly displays the interferometric fringe patterns with high quality for identification of resonant frequencies and mode shapes, and therefore this method will be adopted in this study.

The electrical impedance is a distinguishing characteristic for piezoelectric elements, and the experimental measurement of resonant frequencies for the pure piezoelectric materials is generally performed by impedance analysis. Unfortunately, the resonant frequencies identified by impedance analysis are limited to some specific modes. In this study, the full-field AF-ESPI technique and the point-wise LDV technique are employed to determine the resonant frequencies and mode shapes of a vibrating piezoelectric disc and a multilayer piezoelectric stack actuator with free boundary condition. In addition, in light of the results presented in this work, numerical computations based on the finite element method (FEM) utilizing ABAQUS commercial software package [13] is also made. The resonant frequencies measured by AF-ESPI are compared with those obtained by another two experimental techniques, impedance analysis and LDV, and with those predicted by FEM. The corresponding mode shapes obtained by AF-ESPI and predicted by FEM are also presented for comparisons. The excellent agreement of the numerical results in resonant frequencies and mode shapes with experimental results for a single-layer piezoelectric disc reveals that the proposed methodology are capable of measuring vibration response of piezoelectric materials with satisfactory accuracy. For the case of multilayer piezoelectric stack actuator, the analysis is getting more complicated and there are many unexplored issues should be addressed and will be discussed in detail.

2. THEORY OF AF-ESPI METHOD

The most familiar technique of ESPI used for vibration analysis is the time-averaging method with an image sensor (most commonly using a CCD array) integrating the speckle interferogram field pixel by pixel during a camera's frame period. The name of time-averaging denotes that the vibration measurement includes many periods of object motions during the camera frame period. Two different optical setups are commonly used (out-of-plane sensitivity and in-plane sensitivity) for the vibration measurement. Fundamentals with regards to the AF-ESPI method for in-plane and out-of-plane measurement can be found in Refs. [11,12].

2.1 Out-of-Plane Vibration

When the specimen vibrates periodically, the light intensity of the vibrating image detected by a charge-coupled device (CCD) camera can be expressed by the time-averaging method as

$$I=\frac{1}{\tau}\int_0^{\tau}\left\{I_0+I_R+2\sqrt{I_0 I_R}\cos[\phi+\frac{2\pi}{\lambda}A(1+\cos\theta)\cos\omega t]\right\}dt \tag{1}$$

where I_0 is the object light intensity, I_R is the reference light intensity, $\phi = \phi(x, y)$ is the random phase difference between the object field and the reference field, λ is the wavelength of laser, A is the vibration amplitude, θ is the angle between the object light and the observation direction, τ is the CCD refresh time, and ω is the angular frequency.

Assume that the vibration period is much shorter than the CCD refresh time (i.e. $\tau >> \frac{2\pi}{\omega}$) and let

$$\Gamma=\frac{2\pi}{\lambda}(1+\cos\theta) \tag{2}$$

then, Eq. (1) can be approximated to a simplified form as [6]

$$I_1 = I_0 + I_R + 2\sqrt{I_0 I_R}(\cos\phi)\, J_0(\Gamma A) \tag{3}$$

where J_0 is a zero-order Bessel function of the first kind. As the vibration of specimen goes on, we take the second image by CCD and assume that the vibration

amplitude of the second image has changed from A to $A + \Delta A$ due to the electronic noise or the instability of the apparatus. The light intensity of the second image can be represented as

$$I_2 = \frac{1}{\tau}\int_0^{\tau}\left\{I_0 + I_R + 2\sqrt{I_0 I_R}\cos[\phi + \Gamma(A+\Delta A)\cos\omega t]\right\}dt \tag{4}$$

Expanding Eq. (4) by using the Taylor series expansion; keeping the first two terms and neglecting the higher order terms, we get

$$I_2 = I_0 + I_R + 2\sqrt{I_0 I_R}\,(\cos\phi)\left[1-\frac{1}{4}\Gamma^2(\Delta A)^2\right]J_0(\Gamma A) \tag{5}$$

When these two images, i.e., I_1 and I_2, are subtracted and rectified by the image-processing system, the resulting light intensity can be expressed as

$$I = |I_2 - I_1| = \frac{\sqrt{I_R I_0}}{2}\left|(\cos\phi)\,\Gamma^2(\Delta A)^2\,J_0(\Gamma A)\right| \tag{6}$$

2.2 In-Plane Vibration

Similar to the out-of-plane vibration case, the first and second image intensities, i.e., I_1 and I_2, for in-plane vibration using the time-averaging method are expressed as

$$I_1 = I_0 + I_R + 2\sqrt{I_0 I_R}\,(\cos\phi)\,J_0(\Gamma' A') \tag{7}$$

and

$$I_2 = I_0 + I_R + 2\sqrt{I_0 I_R}\,(\cos\phi)\left[1-\frac{1}{4}\Gamma'^2(\Delta A')^2\right]J_0(\Gamma' A') \tag{8}$$

where I_0 = the object light intensity, I_R = the reference light intensity, A' = vibration amplitude of in-plane vibration, $\Gamma' = 4\pi\sin\theta'/\lambda$, and θ' = half of the angle between two illumination lights. Subtracting (8) from (7) and rectifying by the image processing system, we can obtain image intensity as

$$I = |I_2 - I_1| = \frac{\sqrt{I_R I_O}}{2}\left|(\cos\phi)\,\Gamma'^2\,(\Delta A')^2 J_0(\Gamma' A')\right| \tag{9}$$

From Eqs. (6) and (9), it is interesting to note that the fringe patterns for both the out-of-plane and in-plane vibration motions obtained by AF-ESPI are modulated by the zero-order Bessel function. Combining the out-of-plane and the in-plane optical setups by the AF-ESPI method, we can construct complete vibration characteristics of piezoelectric materials, including resonant frequencies and mode shapes at the same time.

3. EXPERIMENTAL AND NUMERICAL RESULTS

Because the polarized piezoelectric ceramics have the same symmetry as a hexagonal crystal in class C_{6v} = 6mm, it can be modeled as a transversely isotropic material. For a transversely isotropic material referred to a Cartesian coordinate system x_1, x_2, x_3 and assuming that $x_1 - x_2$ is the isotropic plane and x_3 is the poling direction, then the constitutive equation for piezoelectric ceramics are represented in a matrix form as Eq. (10). It is obvious that the complete description of the material characteristic for lead zirconate titanate (PZT) ceramics needs ten material constants; they are five elastic constants (C_{11}^E, C_{12}^E, C_{13}^E, C_{33}^E and C_{44}^E), three piezoelectric constants (e_{15}, e_{31} and e_{15}) and two dielectric constants (ε_{11}^s and ε_{33}^s).

In this section, the vibration characteristics of a single-layer piezoelectric disc and a multilayer piezoelectric stack actuator are investigated. The experimental and numerical results are divided into two parts according to the category of the single-layer results and the multilayered results.

(1) The results of the single-layer piezoelectric disc

The single-layer piezoelectric disc with completely free boundary is analyzed first. The diameter and thickness of this piezoelectric disc are 20mm and 1mm, respectively. This piezoelectric disc is made of $Pb(Zr\cdot Ti)O_3$ ceramics, and the model number is PIC-151 (Physik Instrumente, Germany). The material properties of this thin piezoelectric disc are listed in Table 1. The polarization axis is in the x_3 direction, and two opposite faces (x_1-x_3 plane) of the piezoelectric disc are completely coated with silver electrodes. The single-layer piezoelectric disc has the completely

$$\begin{bmatrix} T_1 \\ T_2 \\ T_3 \\ T_4 \\ T_5 \\ T_6 \\ D_1 \\ D_2 \\ D_3 \end{bmatrix} = \begin{bmatrix} C_{11}^E & C_{12}^E & C_{13}^E & 0 & 0 & 0 & 0 & 0 & -e_{31} \\ C_{12}^E & C_{11}^E & C_{13}^E & 0 & 0 & 0 & 0 & 0 & -e_{31} \\ C_{13}^E & C_{13}^E & C_{33}^E & 0 & 0 & 0 & 0 & 0 & -e_{33} \\ 0 & 0 & 0 & C_{44}^E & 0 & 0 & 0 & -e_{15} & 0 \\ 0 & 0 & 0 & 0 & C_{44}^E & 0 & -e_{15} & 0 & 0 \\ 0 & 0 & 0 & 0 & 0 & (C_{11}^E - C_{12}^E)/2 & 0 & 0 & 0 \\ 0 & 0 & 0 & 0 & e_{15} & 0 & \varepsilon_{11}^s & 0 & 0 \\ 0 & 0 & 0 & e_{15} & 0 & 0 & 0 & \varepsilon_{11}^s & 0 \\ e_{31} & e_{31} & e_{33} & 0 & 0 & 0 & 0 & 0 & \varepsilon_{33}^s \end{bmatrix} \begin{bmatrix} S_1 \\ S_2 \\ S_3 \\ S_4 \\ S_5 \\ S_6 \\ E_1 \\ E_2 \\ E_3 \end{bmatrix} \tag{10}$$

stress-free boundary condition and is excited by the application of an AC voltage across electrodes on the two surfaces. A self-arranged time-averaging ESPI system is used to perform the experimental measurements for resonant frequencies and corresponding full field mode shapes. The optical layout of the AF-ESPI systems, as shown in Fig. 1 and Fig. 2, is used to perform the out-of-plane and in-plane measurements for resonant frequencies and corresponding mode shapes. A He-Ne laser (Melles Griot 05-LHP-928) with 35mW and wavelength λ = 632.8nm is used as the coherent light source. Detailed experimental procedures of the AF-ESPI technique for vibration measurement are performed as follows. First, a reference image is taken after the specimen vibrates with the second image taken subsequently, the reference image is subtracted by the image processing system. If the vibrating frequency is not at the resonant frequency, only randomly distributed speckles are displayed and no fringe patterns will be shown. However, if the vibrating frequency is in the neighborhood of the resonant frequency, distinct stationary fringe patterns will be observed in the monitor. From the aforementioned experimental procedures, the resonant frequencies and the corresponding full-field mode shapes can be determined at the same time by using the AF-ESPI technique.

Table 1 Material properties of PIC-151 piezoelectric ceramics

Quality	PIC-151
C_{11}^E (N/m^2)	10.76×10^{10}
C_{12}^E	6.313×10^{10}
C_{13}^E	6.386×10^{10}
C_{33}^E	10.04×10^{10}
C_{44}^E	1.962×10^{10}
C_{66}^E	2.224×10^{10}
e_{31} (N/Vm)	-9.52
e_{33}	15.14
e_{15}	11.97
ρ (Kg/m^3)	7800
$\varepsilon_{11}^s/\varepsilon_0$	1111
$\varepsilon_{33}^s/\varepsilon_0$	925
ε_0	8.85×10^{-12}

In addition to the experimental measurements, numerical computations of resonant frequencies as well as mode shapes are also implemented by commercially available software ABAQUS finite element package, in which three-dimensional 20-node solid piezoelectric elements (C3D20RE) are selected to analyze the problem.

Figure 3 shows the detailed out-of-plane and in-plane mode shapes of the PIC-151 piezoelectric disc obtained by AF-ESPI and FEM at completely free boundary condition. It is worthy to note that although the area of the piezoelectric disc is small (only 20mm in diameter), the AF-ESPI optical system is capable of obtaining good quality of the interferometric fringe pattern. For finite element results as shown in the right hand side of Fig. 3, dashed lines and the symbol " – " are used to indicate the concave displacements, while solid lines and the symbol "+" are used to denote the convex displacements. The transition from solid lines to dashed lines corresponds to a zero displacement line, or a nodal line that is represented as a bold black line. The zero-order fringe, which is the brightest fringe on experimental results, represents the nodal lines of the piezoelectric disc at resonant frequencies. The rest of the fringes are contours of constant amplitudes of displacement. The mode shapes obtained by experimental results can be checked by the nodal lines and fringe patterns with the numerical finite element calculations. Excellent agreements of the experimental measurements and numerical computations on the vibration mode shapes are found for all the vibration modes in the single-layer piezoelectric disc, including the out-of-plane and in-plane modes.

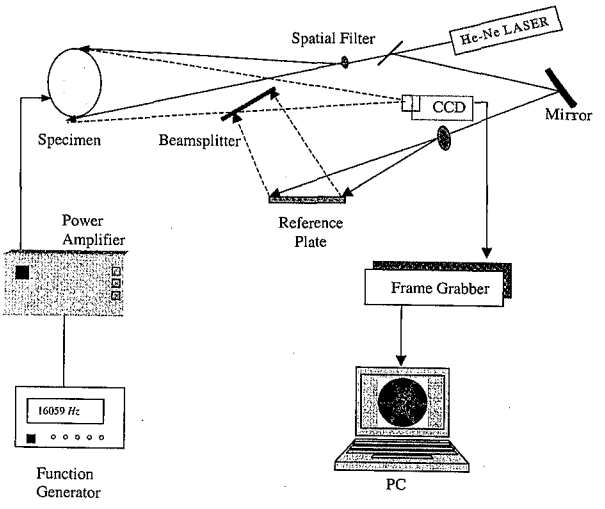

Fig. 1 Optical setup with out-of-plane sensitivity for ESPI

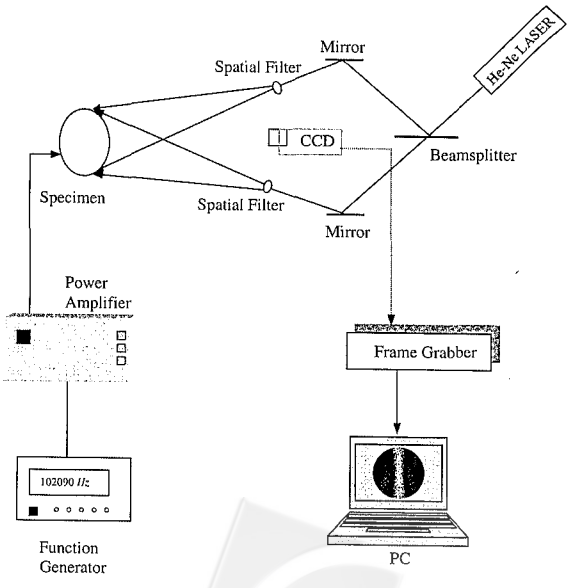

Fig. 2 Optical setup with in-plane sensitivity for ESPI

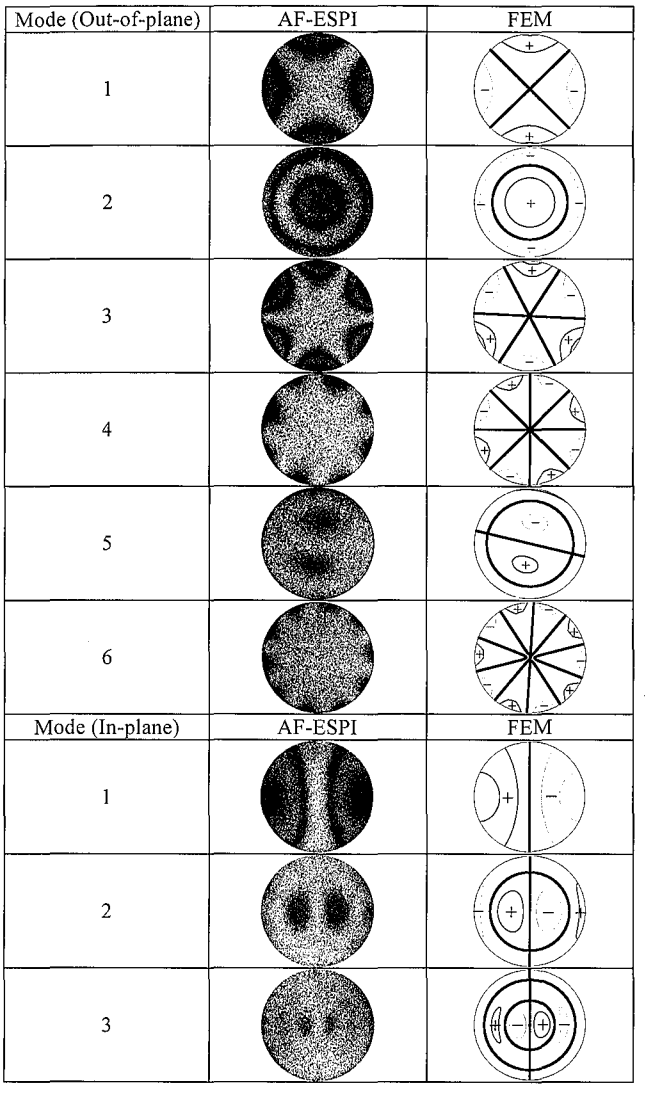

Fig. 3 Mode shapes obtained by AF-ESPI and FEM for a PIC-151 piezoelectric disc

Because the electrical impedance will drop to a local minimum when it vibrates at a resonant frequency, the resonant frequencies can also be obtained by the impedance analysis. Figure 4 shows the impedance curve of this piezoelectric disc measured by a HP4194A impedance/gain-phase analyzer. The local minimum appearing in the impedance curve corresponds to resonance. Because the summation of the induced charge distributed over the electrode surfaces is zero for out-of-plane modes, so only the in-plane modes can be measured by the impedance analysis.

The second experimental optical method, the laser Doppler vibrometer (LDV) which is a point-wise displacement measurement technique, is used to investigate the vibration characteristics of the single-layer piezoelectric disc and multilayer piezoelectric stack actuator. The optical system is based on the principle of Michelson interferometer and the Doppler effect. A built-in dynamic signal analyzer (DSA) is integrated into the LDV system to become the LDV-DSA system. The DSA unit is composed of an analysis software and a plug-in waveform generator board that can provide the swept-sine excitation signal. In the analysis software, the swept-sine excitation signal is taken as input and the response measured by LDV is conversed into the voltage signal and is taken as output. After the fast Fourier transform (FFT) processing of the input and output with the DSA software, the ratio of output/input ("gain") is obtained. The result chart that shows the frequency response curve can be obtained. The peak values appearing in the frequency response curve are the resonant frequencies. Figure 5 indicates the frequency response curve of the single-layer piezoelectric disc obtained by the LDV-DSA system. A detailed description of LDV-DSA system and the working principle can be found in Refs. [14,15].

Table 2 tabulates the out-of-plane and in-plane resonant frequencies obtained by AF-ESPI, impedance analysis, LDV and FEM methods. It is worthy to note that the resonant frequencies for the out-of-plane modes measured by the AF-ESPI and LDV are in good agreement. Excellent agreements for the in-plane modes are obtained by AF-ESPI and Impedance. The percentage of error between three experimental measurements and finite element results are also shown in Table 2. The largest error is 6.28% and the average error in the results is 3.87%. This discrepancy may be due to the interference of conducting wires, the thickness variations across the disc, the experimental

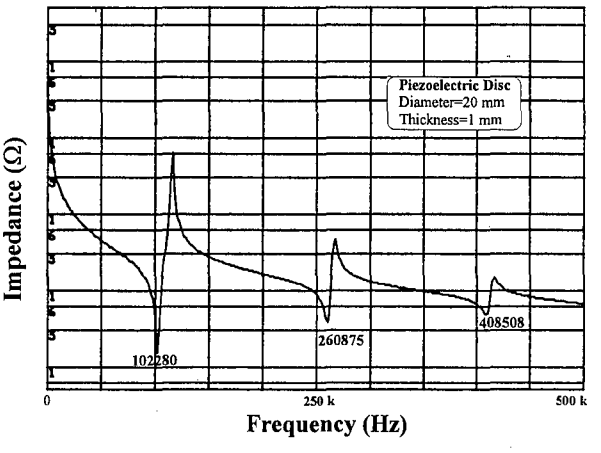

Fig. 4 Impedance curve of the PIC-151 piezoelectric disc

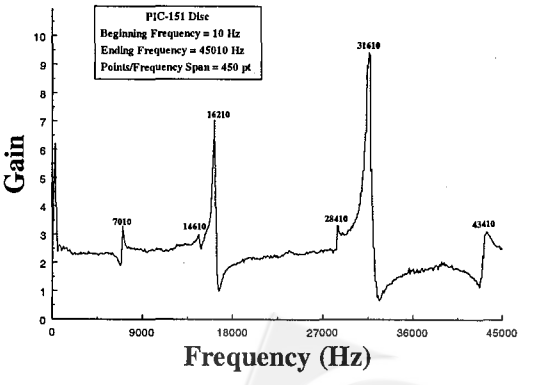

Fig. 5 Frequency response curve measured by LDV of the PIC-151 piezoelectric disc

determination of resonant frequencies, errors in finite element solutions and the material constants measurement. It is concluded that the measured results including the mode shapes and corresponding resonant frequencies are in good agreement with that predicted by FEM computation for the single-layer piezoelectric disc.

Table 2 Resonant frequencies for a single layer PIC-151 piezoelectric disc

Mode (Out-of-plane)	AF-ESPI (Error %)	LDV (Error %)	Impedance (Error %)	FEM (Hz)
1	6895 (– 3.31)	7010 (– 1.69)	–	7131
2	14630 (– 6.15)	14610 (– 6.28)	–	15589
3	16059 (– 3.33)	16210 (– 2.42)	–	16612
4	28194 (– 2.97)	28410 (– 2.22)	–	29056
5	31537 (– 5.28)	31610 (– 5.06)	–	33294
6	43223 (– 2.31)	43410 (– 1.89)	–	44244
Mode (In-plane)	AF-ESPI (Error %)	–	Impedance (Error %)	FEM (Hz)
1	102090 (5.80)	–	102280 (5.99)	96497
2	260430 (4.02)	–	260875 (4.19)	250374
3	408072 (3.37)	–	408508 (3.48)	394774

(2) The results of the multilayer piezoelectric stack actuator

The multilayer piezoelectric stack actuator is composed of individual lead zirconate titanate (PZT) ceramic discs, electrically insulated ceramics and connecting metal electrodes. These piezoelectric elements have widely used in many industrial applications. The investigation on the vibration analysis of a multilayer piezoelectric stack actuator will be presented and discussed in detail. The multilayer piezoelectric stack actuator is a bare stack actuator that is manufactured by Piezomechanik Inc.; the model number is PSt 1000/25/5. Figure 6 shows its schematic illustration of this specimen; two wear resistant ceramics and ten contacted layers of PZT piezoelectric ceramics are connected by adhesives. The properties of the PZT ceramics are very similar to those of PZT-5A. The contact of each piezoelectric disc during pile up is done by introducing thin metal sheet between the layers. The detailed material constants of the wear resistant ceramics and PZT ceramics are listed in Table 3. To simplify this problem in FEM simulation, it is assumed that the discrete layers of each piezoelectric disc in the multilayer piezoelectric stack actuator are perfectly bonded, and the effect of thin metal electrodes is neglected. Figure 7 shows the impedance curve of this multilayer piezoelectric stack actuator measured by the HP4194A. Table 4 lists the resonant frequencies

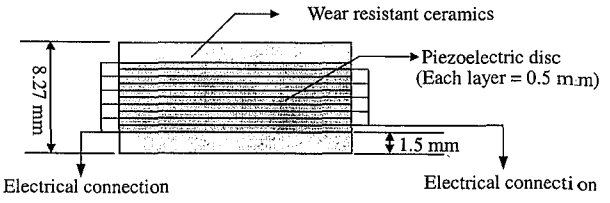

Fig. 6 Schematic illustration of specimen configuration for the multilayer piezoelectric stack actuator

Table 3 Material properties of wear resistant ceramics and PZT-5A ceramics

Quality	Wear Resistant Ceramics	Quality	PZT Ceramics
E (N/m^2)	100×10^9	C_{11}^E (N/m^2)	12.035×10^{10}
		C_{12}^E	7.518×10^{10}
ν	0.22	C_{13}^E	7.509×10^{10}
ρ (Kg/m^3)	3650	C_{33}^E	11.087×10^{10}
		C_{44}^E	2.153×10^{10}
		C_{66}^E	2.257×10^{10}
		e_{31} (N/Vm)	– 5.35
		e_{33}	18.70
		e_{15}	12.30
		ρ (Kg/m^3)	7500
		$\varepsilon_{11}^S/\varepsilon_0$	919
		$\varepsilon_{33}^S/\varepsilon_0$	827
		ε_0	8.85×10^{-12}

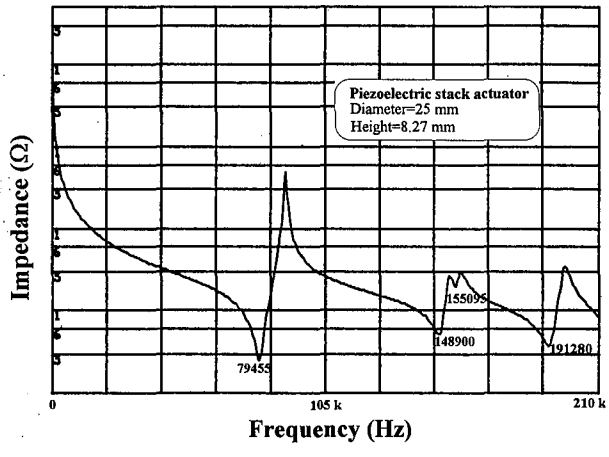

Fig. 7 Impedance curve of the multilayer piezoelectric stack actuator

Table 4 Resonant frequencies for a multilayer piezoelectric stack actuator

Mode	AF-ESPI (Hz)	LDV Input=10V	LDV Input=1V	Impedance (Hz)	FEM (Hz)
1	85410	87710	79910	79545	107683
2	150310	151510	148710	148900	152099
3	155876	156310	155610	155095	164413
4	194345	196210	191010	191280	210270

obtained by AF-ESPI, LDV, impedance analysis and FEM. It is found that the measured resonant frequencies by AF-ESPI are larger than those obtained by impedance analysis and the difference between these two results is large. This observation is different from that presented in Table 2 for the single-layer piezoelectric disc. In order to have a better understanding of the reason that causes the discrepancies of resonant frequencies, the frequency response curve of this multilayer piezoelectric stack actuator obtained by the LDV is also shown in Fig. 8. The peak values of this frequency response curve are also indicated in the fourth column of Table 4. We can see that the measured results of resonant frequencies by LDV and impedance analysis agree very well. It is noted that the default value of the input AC exciting level is set to be 1V for both LDV and impedance analysis. However, the AC exciting level is generally amplified and a higher level should be provided to obtain interferometric fringes in AF-ESPI. Hence the variation in measured values of resonant frequencies for AF-ESPI and impedance may be attributed to the differences of input exciting level in different experimental techniques. In order to verify the effect of input exciting level on resonant frequencies for multilayer piezoelectric stack actuator, the exciting level of the LDV is amplified to 10V and the corresponding frequency response curve is shown in Fig. 9. The resonant frequencies are indicated in the third column of Table 4, which agree with the results obtained by AF-ESPI method. It is clearly indicated that the resonant frequencies of the multilayer stack actuator increase as the AC input exciting level is amplified. Hence the dynamic behavior of the multilayer piezoelectric stack actuator is different at high and low AC excitation voltage level. Because the conversion of electric energy into the mechanical energy is not complete at high AC electrical fields, the heat is induced and an internal stress is generated under high AC electrical fields which lead to the shift in resonant frequencies.

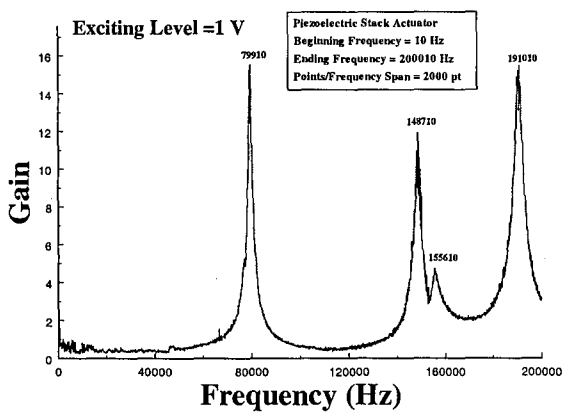

Fig. 8 Frequency response curve measured by LDV of the multilayer piezoelectric stack actuator for the driving voltage of 1V

As shown in Fig. 6 that the thickness and the diameter of the multilayer piezoelectric stack actuator are 8.27mm and 25mm, respectively, hence the out-of-plane and in-plane motions are coupled for each mode. The corresponding out-of-plane and in-plane mode shapes measured by AF-ESPI and predicted by FEM are shown in Fig. 10. It is found that the mode shapes of mode 1 to mode 4 have similar patterns in AF-ESPI and FEM results, but the out-of-plane mode shapes for mode 1 and mode 2 are slightly eccentric. It may be due to the debonding of these plies of ceramics and improper manufacture process of the specimen. Furthermore, the in-plane mode shape of mode 2 is not clear and the mode 3 in AF-ESPI results is not found. This can be attributed to the fact that the induced in-plane vibration amplitudes in these two modes are smaller than the resolution of the AF-ESPI. A larger discrepancy in resonant frequencies and mode shapes is found for the experimental measurements and FEM calculations because of the complexity of the multilayer piezoelectric stack actuator.

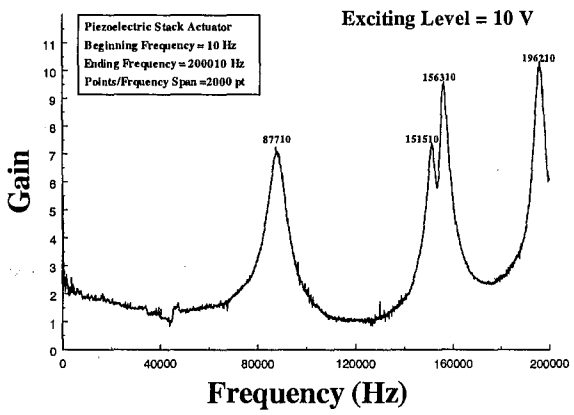

Fig. 9 Frequency response curve measured by LDV of the multilayer piezoelectric stack actuator for the driving voltage of 10V

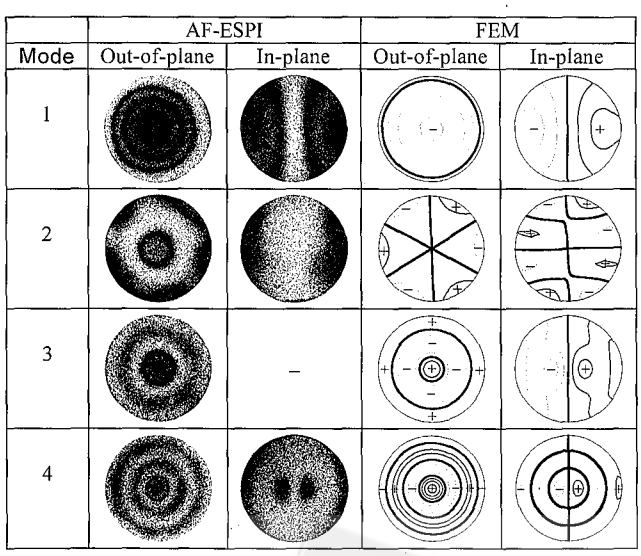

Fig. 10 Mode shapes obtained by AF-ESPI and FEM for the multilayer piezoelectric stack actuator

4. CONCLUSIONS

It is known that the vibration characteristics of piezoelectric discs have important applications in many engineering fields. However, there are only very few experimental results available for vibrating piezoelectric discs. Existing experimental techniques for the multilayer piezoelectric stack actuator are commonly used to obtain the static and dynamic responses at specific points. Very few investigations on the vibration characteristics for the piezoelectric stack actuator are found in the literature. In this study, experimental measurements on vibration characteristics for single-layer piezoelectric disc and multilayer piezoelectric stack actuator are presented. The resonant frequencies and mode shapes of vibrating piezoelectric discs in resonance are investigated by using three experimental techniques (AF-ESPI, LDV and impedance) and FEM method. It is shown that the AF-ESPI method, compared with other techniques, has the advantages of non-contact, full-field, real-time and high-resolution measurement for the vibration analysis of piezoelectric discs. The resonant frequencies and full-field mode shapes measured by AF-ESPI correlate well with FEM for the single-layer piezoelectric disc. However, discrepancies of the resonant frequencies for the multilayer piezoelectric stack actuator are found for both results. These discrepancies may be due to the complexity of the specimen configuration, material constants measurement and manufacture process. It is found that the excitation voltage level has a significant effect on the resonant frequencies of the multilayer piezoelectric stack actuator. Many unexplored issues for the vibration characteristics of the multilayer piezoelectric stack actuator are addressed and are discussed in detail.

ACKNOWLEDGMENTS

The authors gratefully acknowledge the financial support of this research by the National Science Council (Republic of China) under Grant NSC 90-2212-E-002-163.

REFERENCES

[1] Wolff, A., Cramer, D., Hellebrand, H., Probst, I. and Lubitz, K., "Optical Two Channel Elongation Measurement of PZT Piezoelectric Multilayer Stack Actuators," *Proceedings of the Ninth IEEE International Symposium on Applications of Ferroelectronics*, pp. 755–757 (1994).

[2] Damjanovic, D., "Nonlinear Piezoelectric Response in Ferroelectric Ceramics," *Piezoelectric Materials: Advances in Science, Technology and Applications*, Kluwer Academic Publishers, Netherlands, pp. 123–135 (2000).

[3] Janocha, H. and Clephas, B., "Measurement and Simulation of the Electromechanical Behavior of Piezoelectric Stack Transducers," *Piezoelectric Materials: Advances in Science, Technology and Applications*, Kluwer Academic Publishers, Netherlands, pp. 179–190 (2000).

[4] Moilanen, H. and Leppävuori, S., "Laser Interferometric Measurement of Displacement-Field Characteristics of Piezoelectric Actuators and Actuator Materials," *Sensors and Actuators a Physical*, 92, pp. 326–334 (2001).

[5] Butters, J. N. and Leendertz, J. A., "Speckle Patterns and Holographic Techniques in Engineering Metrology," *Optics and Laser Technology*, 3, pp. 26–30 (1971).

[6] Jones, R. and Wykes, C., *Holographic and Speckle Interferometry*, Cambridge, England: Cambridge University Press, pp. 162–196 (1989).

[7] Wykes, C., "Use of Electronic Speckle Pattern Interferometry (ESPI) in the Measurement of Static and Dynamic Surface Displacements," *Optics and Laser Technology*, 21, pp. 400–406 (1982).

[8] Creath, K. and Gudmunn, A., "Vibration-Observation Techniques for Digital Speckle-Pattern Interferometry," *Journal of the Optical Society of America A*, 2, pp. 1629–1636 (1985).

[9] Nakadate, S., "Vibration Measurement Using Phase-Shifting Speckle Pattern Interferometry," *Applied Optics*, 25, pp. 4162–4167 (1986).

[10] Wang, W. C., Hwang, C. H. and Lin, S. Y., "Vibration Measurement by the Time-Averaging Electronic Speckle Pattern Interferometry Method," *Applied Optics*, 35, pp. 4502–4509 (1996).

[11] Huang, C. H. and Ma, C. C., "Vibration Characteristics for Piezoelectric Cylinders Using Amplitude-Fluctuation Electronic Speckle Pattern Interferometry," *AIAA Journal*, 36, pp. 2262–2268 (1998).

[12] Ma, C. C. and Huang, C. H., "The Investigation of Three-Dimensional Vibration for Piezoelectric Rectangular Parallelepipeds Using the AF-ESPI Method," *IEEE Transactions on Ultrasonics, Ferroelectrics, and Frequency Control*, 48, pp. 142–153 (2001).

[13] *ABAQUS User's Manual*, ver. 5.8, Pawtucket, RI: Hibbit, Karlsson, and Sorensen, Inc. (1998).

[14] Lee, C. K. and Wu, G. Y., "High Performance Doppler Interferometer for Advanced Optical Storage System," *Japanese Journal of Applied Physics*, 38, pp. 1730–1741 (1999).

[15] *AVID User's Manual*, Ahead Optoelectronics, Inc.

(Manuscript received Mar. 13, 2002,
Manuscript revised Apr. 24, 2002,
Accepted for publication May 29, 2002.)